Energy Proceedings
Vol 32, 2023
ISSN 2004-2965

Numerical investigation of thermal performance of swirl generator in a solar water heater

Xingyu Feng[1,2], Nicholas J. Miles[1,2], Guozhen Li[1,2], Zheng Wang[1,2], Philip Hall[1, 3*]

[1]University of Nottingham Ningbo China, Faculty of Science and Engineering, 199 Taikang East Road, Ningbo 315100, Zhejiang, China

[2]Nottingham Ningbo China Beacons of Excellence Research and Innovation Institute, Ningbo 315100, PR China

[3]Zhejiang Provincial Key Laboratory for Carbonaceous Wastes Processing and Process Intensification Research
(*Corresponding author: Philip Hall. Email: Philip.HALL@nottingham.edu.cn)

ABSTRACT

This paper presents a numerical investigation of the potential of a 4-lobed swirl generator for enhancing the thermal performance of an active Solar Water Heater (SWH). The hydro-thermal performance of the generator was thoroughly evaluated using the code ANSYS FLUENT 2021 R1, and the results were validated against available experimental data in the literature. The predicted results demonstrated that the proposed swirl generator was capable of giving a higher Performance Evaluation Criteria (PEC) compared to twisted tape as it enhanced the heat transfer at the expense of a much lower pressure loss than the twisted tapes. However, with only one swirl generator, the PEC value for the swirl generator was only slightly higher than 1 and the analysis with the field synergy principle revealed that the thermal enhancement produced only prevails for 30D to 40D downstream. To achieve optimal thermal enhancement in the SWH, strategic placement regimes were examined by regularly placing 2, 3 and 4 swirl generators, respectively, inside the SWH. Simulation results indicated that, with an optimal placement of the swirl generator, the heat transfer coefficient is increased by 9.9% with an extra pressure drop of 26.9% more than a plain circular tube. This increase in heat transfer coefficient can reduce the overall pumping time and, more importantly, can make the SWH more reliable in moderate weather.

Keywords: solar heat exchanger, 4-lobed swirl generator, twisted tape, decaying swirl flow, CFD Ansys fluent, field synergy principle

NONMENCLATURE

Abbreviations

PEC	Performance Evaluation Criteria
SWH	Solar water heater

Symbols

A	Surface area
c_p	Specific heat capacity
D_h	Hydraulic diameter
f	Friction factor
h	Heat transfer coefficient
L	Length of the tube side
Nu	Nusselt number
Δp	Pressure drop
$\dot{Q}$	Heat transfer rate
q_w	Heat flux
T_f	Fluid temperature
T_w	Wall temperature
∇T	Logarithmic mean temperature
$\vec{U}$	Velocity field
u	Fluid velocity
μ	Viscosity
θ	Synergy angle
ρ	Density

1. INTRODUCTION

Solar thermal energy is one of the most important sources of renewable energy. By the end of 2020, the worldwide capacity of water-based solar thermal systems is 500 GW, corresponding to a final energy savings equivalent to 43.6 million tons of oil. Among which, the vast majority of the total capacity in operation

This is a paper for Applied Energy Symposium 2023: Clean Energy towards Carbon Neutrality (CEN2023), April 23-25, 2023, Ningbo, China.

was installed in China (364.0 GW), accounting for 72.8% of the total installed capacity. In particular, domestic Solar Water Heaters (SWH) had the highest solar heating applications in 2021[1].

Despite its wide applications, problems arise from its low efficiency on cloudy days and fouling issues. Existing passive solutions involved installing swirl devices such as twisted tape and wired coils to enhance the thermal performance of the SWH [2]. For instance, Saravanan et al. [3] reported an 8.4% higher heat transfer rate by inserting v-cut twisted tapes with a ratio of 3 compared with a flat plate solar heater. Sundar et al. [4] studied the combined effect of Al2O3 nanofluid and wired coils, and the collector efficiency was enhanced by 64.15% compared with that of the original flat plate collectors. Farshad et al. [5] numerically investigated the heat transfer behavior of nanofluid in a solar heater with the insertion of multi-channeled twisted tape. However, it has been commonly observed that by inserting a full-length twisted tape, the pressure drop was increased by more than 1.85 times in comparison to an empty tube [6]. Such a high pressure drop further raised the requirements for pumping energy when applying these devices to existing systems. Researchers attempted to reduce the pressure drop by shortening the length of the twisted tape [7] and using regularly spaced short-length twisted tapes [8]. Such alterations showed better Performance Evaluation Criteria (PEC) at Reynolds numbers higher than 10,000. In addition to twisted tapes, the thermal enhancement ability of lobed tubes has also attracted considerable attention. Yang et al. [9] demonstrated the heat transfer enhancement ability of 2-lobed swirl tubes and concluded that the optimal operation regime was at lower Reynolds numbers. Tang et al. [10] compared the thermal performance of 2- and 3-lobed tubes and reported that the 3-lobed one provided a 5.8% higher PEC value than the 2-lobed one. However, a research gap exists in determining whether installing a shorter length lobed tube instead of a full-length lobed tube will still have a positive effect on heat transfer as twisted tapes. Moreover, the fouling issue inside the SWH remains unsolved. Though inserting twisted tape increases heat transfer efficiency, the additional surfaces are prone to fouling and are challenging to clean. Li et al. [11] demonstrated that a 4-lobed swirl tube with a pitch- to-diameter (PD) ratio of 8 is capable of inducing a cleaning effect on the internal pipe surface by producing stronger tangential force, thus has the potential to mitigate fouling problems.

In light of the above review, this paper proposes to use a 4-lobed swirl pipe to improve the thermal performance of the active SWH with minimum pressure loss, which also has the potential to mitigate the fouling problems. The circular pipe that connects the two swirl generators is also crucial because swirl only occurs at the front of the pipe and degrades as it moves downstream. Therefore, this paper attempts to use the field synergy principle [12] to analyse the swirl performance. The Nusselt number, friction factor and PEC of different geometries are predicted and compared. Moreover, 2, 3 and 4 swirl generators are placed regularly inside the SWH to further increase thermal performance.

2. NUMERICAL SIMULATION

2.1 Simulation arrangement and model

Only one heating unit from an active SWH array is modeled, which is shown in Fig. 1. The absorption pipes are a plain circular pipe as a baseline, pipes with inserted twisted tapes, and swirl pipes, respectively, where the swirl generator is the same as proposed by Li et al. [11] while the twisted tape is the same as described by Eiamsa-ard et al. [7] with a twisted ratio of 5.

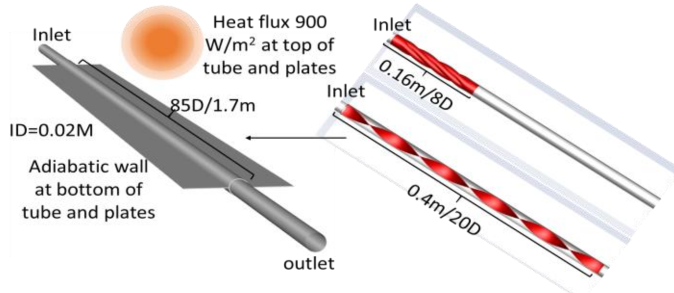

Fig. 1. Solar heater with swirl devices.

The diameter and the length of the absorption tube are 0.02m and 1.7 m, respectively, equaling 85 times the diameter (85D). The tube is made of copper. A constant solar heat flux of 900 W is given on the top part of the tube and absorption plates, representing solar radiation, while the bottom is set as adiabatic. The absorption plate is made of aluminum. The tube is extended 0.5m at both ends of the absorption tube for the flow field to develop. The wall condition for the extended tube is also adiabatic. The inlet temperature is set at 293K, and the velocity ranges from 0.3m/s to 0.8m/s. Water is used as a working fluid and its properties are assumed to be constant [10] as shown in Table 1. The detailed geometrical parameters are shown in Table 2.

Table 1. Water properties.

Density [kg/m^3]	Specific Heat [J/(kg×K)]	Thermal Conductivity [W/(m×K)]	Viscosity [kg/(m×s)]
998.2	4182	0.6	0.001

Table 2. Geometrical parameters.

Parameters	Value [m]
Tube length	2.7m (1.7m+0.5m+0.5m)
Tube diameter	0.02m
Tube and plate thickness	0.001m
Plate width	0.04m

2.2 Thermal performance indicators

The heat transfer rate $\dot{Q}$, Nusselt number, Pressure loss, and Performance Evaluation Criteria (PEC) are used to evaluate the SWH performance. The heat transfer rate $\dot{Q}$ can be calculated from the following equation:

$$\dot{Q} = hA(T_w - T_f)$$

Where A is the surface area where the heat transfer taken place, *h* is the heat transfer coefficient, T_f is the average temperature of the fluid at the inlet and outlet, T_w is the temperature of the wall surface, h is the heat transfer coefficient.

Nusselt number is a dimensionless number that describes the degrade of heat transfer rate.

$$Nu = \frac{hD_h}{\lambda}$$

Where D_h is the hydraulic diameter of the pipe, λ is the thermal conductivity of the fluid.

Reynolds number is a dimensionless number that predicts fluid flow patterns in different situations.

$$Re = \frac{\rho u D_h}{\mu}$$

Where μ is the viscosity of the fluid, ρ is the density, u is the velocity.

Pressure drop in different geometries can be calculated by following equations:

$$\Delta p = f\frac{L}{D_h}\frac{\rho u^2}{2}$$

Where L is the length of the tube side, f is the friction factor.

References [9] used PEC (performance evaluation criteria) to evaluate the hydro-thermal performance of the devices. Here, this factor is used to compare the heat transfer coefficient and pressure drop between the swirl generator and circular tube under the same operational conditions.

$$PEC = \frac{Nu_s/Nu_c}{(f_s/f_c)^{1/3}}$$

2.3 Mesh test and validation

Commercial computational fluid dynamics software ANSYS FLUENT 2021 R1 was used for the simulation. Fluent meshing is used to create a polyhedral mesh, as shown in Fig. 2. To simplify the problem, it is assumed that the flow is continuous, steady and in turbulence regions. SST k-ω model is selected since it produces more accurate results in swirl pipe [10]. For all simulations, the y^+ values were maintained around 1. The SIMPLEC was employed for pressure-velocity coupling and the second order upwind scheme was used for all viscous terms. The criteria for all residuals was at 10-6 . During the calculation, the total pressure at the inlet, the static temperature at the outlet, and the energy balances were all monitored.

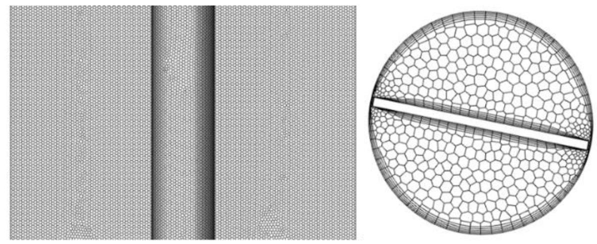

Fig. 2. Mesh overview.

A mesh independence test was utilized to reduce the inaccuracies caused by mesh density. Table 3 demonstrates various mesh sizes and the corresponding results for the Nusselt number and friction factor. The fine mesh is selected to carry out further simulations.

Table 3. mesh test at Re = 7960.

Mesh	Cell number	Nu	f
Coarse	1176087	74.94	0.0329
Normal	2342231	72.32	0.0331
fine	3508375	71.92	0.0333
Very fine	4674519	71.79	0.0333

The CFD model is validated against experimental results [7] in terms of the Nusselt number and demonstrates good accuracy. The validation geometry is the same as the experimental condition studied by Eiamsa-ard et al. [7] where, as can be seen in Fig. 3, a single tube with twisted tape at a twisted ratio of 5 is inserted inside a circular tube. The heat transfer is achieved by applying a uniform heat flux in the 60D region after the twisted tape.

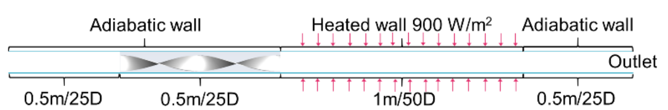

Fig. 3. Boundary condition for validations

As can be seen in Fig. 4, the simulation results of the Nusselt number agree well with the experimental results. The maximum deviation is 9.8% at the lowest Reynolds number. Thus, the heat transfer results produced from simulations are reliable. This validated model is therefore used for simulating the SWH.

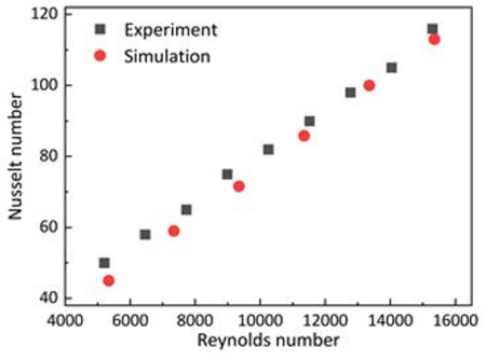

Fig. 4. Validation with experimental results [7].

3. RESULTS AND DISCUSSION

3.1 Thermal performance

The Nusselt number difference for the plain circular pipe, the twisted tape and the swirl pipe is shown in Fig. 5. On average, the Nusselt number for the swirl pipe is 2.0% higher and the twisted tape is 10.8% higher than the circular pipe.

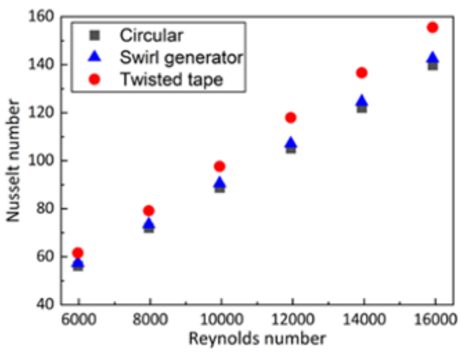

Fig. 5. Nusselt number for two devices

The friction factor difference for twisted tape and the swirl pipe is shown in Fig. 6. On average, the friction factor for the swirl generator is 6.6% higher and for the twisted tape is 65.0% higher than that of the circular one.

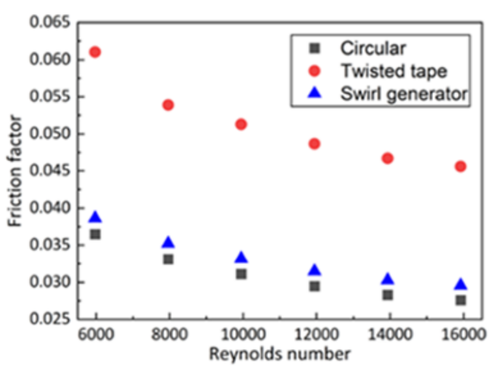

Fig. 6. Friction factor for two devices

The PEC value for two devices is shown in Fig. 7. Due to the high friction factor in twisted tape, the PEC factor for twisted tape is considerably lower than the one for swirl generators. However, PEC values for the swirl generator are only slightly higher than 1, which will further decrease with the increment in Reynolds number. Therefore, it is necessary to attempt different variations to achieve a promising thermal enhancement value, as both devices fail to do so.

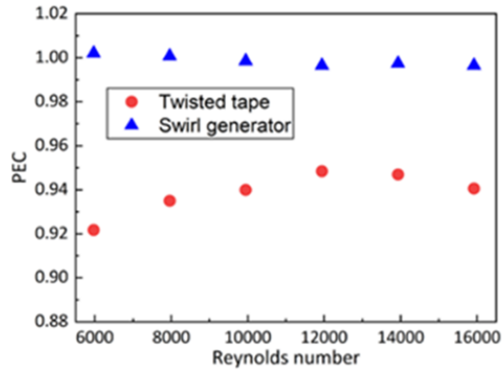

Fig. 7. PEC for two devices

3.2 Field synergy principle

This principle is a theory [12] that explains the thermal enhancement mechanism. Many studies apply this principle to investigate the mechanism in swirl flow devices [9, 10]. It uses the intersectional angle between the temperature gradient and velocity vector to relate the heat transfer efficiency. Through this method, a smaller angle indicates a better heat transfer rate since the flow of momentum is in the same direction as the flow of energy.

$$\int_0^{\delta_t} \rho c_p\left(\left|\vec{U}\right|\left|\nabla T\right| cos\theta\right) dy = q_w$$

To visualize the thermal enhancement effect, the cross-sectional view of the tangential velocity vector and isotherm lines is shown in Fig. 8. In the case of twisted tape, the flow rotation and the disruption of the temperature isotherm line are both mostly around the twisted direction of the tape. On the other hand, the swirl generator produces four obvious vortices that redistribute the temperature and the velocity field.

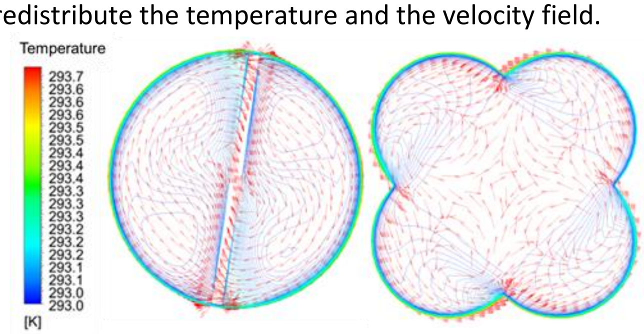

Fig. 8. Velocity vector and isotherm line.

The synergy angle variation for twisted tape and swirl generator is shown in Fig. 9. The synergy angle for the twisted tape is lower than the one for the swirl generator, which explains a lower Nusselt number for swirl pipe in Fig. 5. However, at the downstream end of the swirl section, the thermal enhancement produced by these two swirl flow devices both quickly diminish and reach a certain constant after 50D.

Moreover, the synergy angle variation downstream of the devices seems to fit an exponential trend. An attempt is made to fit an exponential correlation between distance and synergy angle

$$\theta = -\Delta\theta e^{-\gamma\frac{x}{D}} + \theta_c$$

Where θ is the local synergy angle, $\Delta\theta$ is the difference between θ_0 and θ_c when $\frac{x}{D} = 0$, γ is the swirl decaying rate related to synergy angle.

The R^2 values for both correlations can reach 0.98, which indicates that the correlation can generally describe the synergy angle trend for both swirl devices. However, further research on the meaning of the constants in the correlation is required.

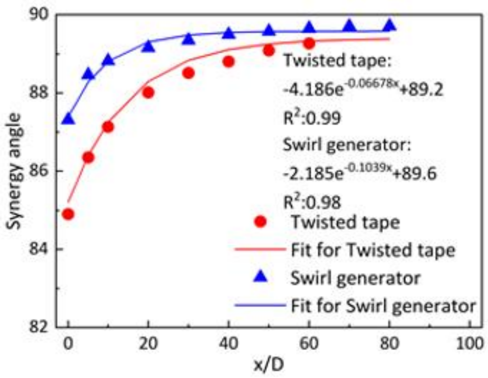

Fig. 9. Synergy angle for two devices

3.3 *Strategic placements of swirl pipes*

Enlighted by the regularly-spaced twisted tape [8], strategic placement schemes for swirl generators are proposed. Similar to regularly-spaced tape, the swirl generator is also regularly spaced within the 85D absorption pipe. In total, four types of arrangements are constructed. Those arrangements are shown in Table 4.

The Nusselt number for different arrangements is shown in Fig. 10. Increasing the number of swirl generators will also enhance the heat transfer rate. The Nusselt number for case 4 enhances 9.9% in comparison with the circular one, which is close to the one for the twisted tape. Those inserted swirl generators create vortexes that prevent the swirl from decaying, which enhances the heat transfer coefficient.

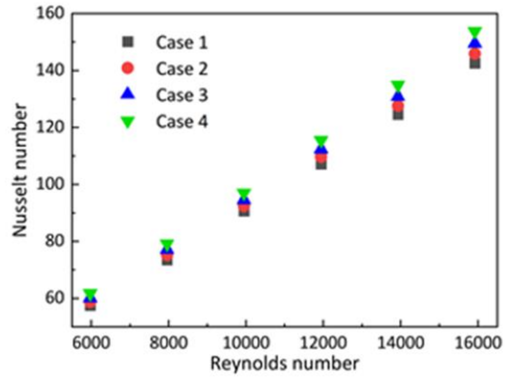

Fig. 10. Nusselt number for different arrangements.

The Friction factor for different arrangements is shown in Fig. 11. Not surprisingly, increasing the amount of swirl generators also leads to higher friction loss due to the creation of turbulence inside the flow. The pressure drops for case 4 augments 26.9%, which is lower than the one for the twisted tape.

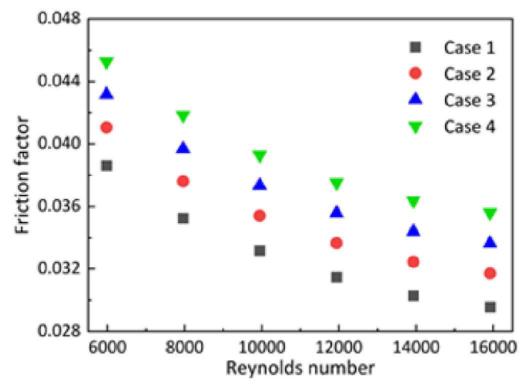

Fig. 11. Friction factor for different arrangements.

The PEC value for different arrangements is shown in Fig. 12. The PEC value also augments when a larger number of swirl generators is inserted. Due to the relatively low pressure drop penalties of swirl generator insertion, the thermal enhancement is not negated. The highest PEC value is achieved in case 4, with an average value of 1.5%.

Table 4. Arrangements illustrations.

Case number	Swirl arrangements
Case 1	Swirl(0.16m)+Circular(1.54m)
Case 2	Swirl(0.16m)+Circular(0.69m)+Swirl(0.16m)+Circular(0.69m)
Case 3	Swirl(0.16m)+Circular(0.407m)+Swirl(0.16m)+Circular(0.407m)+Swirl(0.16m)+circular(0.407m)
Case 4	Swirl(0.16m)+Circular(0.265m)+Swirl(0.16m)+Circular(0.265m)+Swirl(0.16m)+Circular(0.265m)+ Swirl(0.16m)+circular(0.265m)

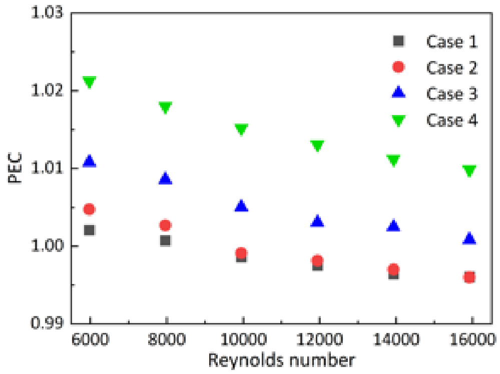

Fig. 12. PEC value for different arrangements.

4. CONCLUSIONS

In this study, the thermal performance of the swirl generator in a SWH was numerically investigated. In the first stage of the investigation, the performance of a swirl generator and a shortened twisted tape were compared. However, both devices gave a relatively low PEC value and twisted tape gave lower one due high pressure drop penalty (65% compared with a circular tube). Through the analysis of the field synergy angle, the reasons for the low performance were high pressure drop and rapid deterioration of the swirl effect. To cope with these issues, different strategic placements of the swirl generator were proposed. With the optimal one, the Nusselt number was increased by 9.9%. The highest PEC value was achieved in case 4, with an average value of 1.5%. Therefore, it is a promising alternative for improving SWH performance.

ACKNOWLEDGEMENT

The authors would like to acknowledge the support from Ningbo Science and Technology Bureau (2022Z157), UNNC Education Foundation - LDS Innovation Fellowship, Zhejiang Provincial Key Laboratory for Carbonaceous Wastes Processing and Process Intensification Research funded by the Zhejiang Provincial Department of Science and Technology (2020E10018).

DECLARATION OF INTEREST STATEMENT

The authors declare that they have no known competing financial interests or personal relationships that could have appeared to influence the work reported in this paper. All authors read and approved the final manuscript.

REFERENCE

[1] Weiss, W.S.-D., M. Solar Heat Worldwide. 2022 [cited 2023 5th March]; Retrieved from: https://www.iea-shc.org/solar-heat-worldwide.

[2] Vengadesan, E.,R. Senthil, A review on recent development of thermal performance enhancement methods of flat plate solar water heater. Solar Energy 2020;206:935-961.

[3] Saravanan, A.,S. Jaisankar, Heat transfer augmentation techniques in forced flow V-trough solar collector equipped with V-cut and square cut twisted tape. International Journal of Thermal Sciences 2019;140:59-70.

[4] Sundar, L.S., Y.T. Sintie, Z. Said, M.K. Singh, V. Punnaiah,A.C.M. Sousa, Energy, efficiency, economic impact, and heat transfer aspects of solar flat plate collector with Al2O3 nanofluids and wire coil with core rod inserts. Sustainable Energy Technologies and Assessments 2020;40:100772.

[5] Farshad, S.A.,M. Sheikholeslami, Simulation of exergy loss of nanomaterial through a solar heat exchanger with insertion of multi-channel twisted tape. Journal of Thermal Analysis and Calorimetry 2019;138:795-804.

[6] Liu, S.,M. Sakr, A comprehensive review on passive heat transfer enhancements in pipe exchangers. Renewable and Sustainable Energy Reviews 2013;19:64-81.

[7] Eiamsa-ard, S.,P. Seemawute, Decaying swirl flow in round tubes with short-length twisted tapes. International Communications in Heat and Mass Transfer 2012;39:649-656.

[8] Wang, Y., M. Hou, X. Deng, L. Li, C. Huang, H. Huang, G. Zhang, C. Chen,W. Huang, Configuration optimization of regularly spaced short-length twisted tape in a circular tube to enhance turbulent heat transfer using CFD modeling. Applied Thermal Engineering 2011;31:1141-1149.

[9] Yang, S., L. Zhang,H. Xu, Experimental study on convective heat transfer and flow resistance characteristics of water flow in twisted elliptical tubes. Applied Thermal Engineering 2011;31:2981-2991.

[10] Tang, X., X. Dai,D. Zhu, Experimental and numerical investigation of convective heat transfer and fluid flow in twisted spiral tube. International Journal of Heat and Mass Transfer 2015;90:523-541.

[11] Li, G., P. Hall, N. Miles,T. Wu, Improving the efficiency of 'Clean-In-Place' procedures using a four-lobed swirl pipe: A numerical investigation. Computers & Fluids 2015;108:116-128.

[12] Guo, Z.Y., D.Y. Li,B.X. Wang, A novel concept for convective heat transfer enhancement. International Journal of Heat and Mass Transfer 1998;41:2221-2225.